

U-Pb and Ar/Ar ages from the Bonaparte mine, southern British Columbia: Late Middle Jurassic Au ± Cu vein mineralization

Richard M. Friedman¹, Janet E. Gabites¹, and James M. Logan^{2, a}

¹ Pacific Centre for Isotopic and Geochemical Research, Department of Earth, Ocean and Atmospheric Sciences, University of British Columbia, Vancouver, BC, V6T 1Z4

² British Columbia Geological Survey, Ministry of Energy and Mines, Victoria, BC, V8W 9N3

^a corresponding author: Jim.Logan@gov.bc.ca

Recommended citation: Friedman, R.M., Gabites, J.E., and Logan, J.M., 2014. U-Pb and Ar/Ar ages from the Bonaparte mine, southern British Columbia: Late Middle Jurassic Au ± Cu vein mineralization. In: Geological Fieldwork 2013, British Columbia Ministry of Energy and Mines, British Columbia Geological Survey Paper 2014-1, pp. 59-66.

Abstract

An erosional window in the Miocene Chilcotin Group basalt blanket exposes deformed Jurassic monzodiorite and porphyritic quartz diorite on the Bonaparte Plateau, 38 km north of Kamloops. These plutonic rocks host at least eight separate, metre- to cm-wide Au-Cu quartz veins at the Bonaparte mine. Intrusion and mineralization appear to have coincided temporally and spatially with motion along a greenschist-grade, north-trending reverse (east side-up) shear zone. Based on its position along the Wildhorse-Takomkane intrusive belt, we previously assumed that the Bonaparte complex was ~ 195 Ma. However, new U-Pb zircon crystallization ages demonstrate that parts are significantly younger. These data indicate at least two magmatic events: Early Jurassic (~ 189 Ma) for the monzodiorite and Middle Jurassic (~ 166 Ma) for the quartz diorite. Hydrothermal muscovite associated with late stage copper-arsenopyrite-gold mineralization yields an ⁴⁰Ar/³⁹Ar cooling age of 160.4 ± 2.4 Ma linking mineralization to the ~ 166 Ma episode.

Keywords: Zircon crystallization ages, ⁴⁰Ar/³⁹Ar cooling ages, calcalkaline diorite porphyries, gold quartz veins, chalcopyrite, quartz stockwork, potassic, synkinematic alteration and mineralization, Middle Jurassic

1. Introduction

The Bonaparte gold mine (WestKam Gold Corporation) is approximately 38 km north of Kamloops, B.C., straddling map sheets 92I/16W & 92P/1W, at about 51° 02' N and 128° 28' W (Fig. 1). Mineralization at Bonaparte includes intrusion-hosted Au-Cu quartz veins and W-Mo quartz stockworks (Figs. 1, 2; MINFILE 92I-50; Peatfield, 1986; Durfeld, 1980; Logan and Mihalyuk, 2013). Lacking geochronologic control, Logan and Mihalyuk (2013) assumed that the Bonaparte intrusive complex was Jurassic, based on its position in the Wildhorse-Takomkane magmatic belt of Breitsprecher et al. (2010) and Anderson et al. (2010; Fig. 2). To test this correlation, we collected samples of quartz diorite and monzodiorite for U-Pb zircon geochronology, and a sample of sericite-altered intrusion associated with quartz-carbonate veins and gold mineralization for Ar⁴⁰-Ar³⁹ analysis. Results presented herein demonstrate that magmatism (~ 189 Ma monzodiorite and ~ 166 Ma quartz diorite) and mineralization (~ 160 Ma) are significantly younger than in the Wildhorse-Takomkane magmatic belt, precluding correlation. Mineralization at Bonaparte appears to be related to emplacement of ~ 166 Ma quartz diorite.

2. Regional setting

As described by Logan and Mihalyuk (2013), the oldest rocks at the Bonaparte property include a succession of rusty-weathering, graphitic, and siliceous sedimentary rocks of uncertain age. This succession has been correlated with the Carboniferous to Permian Harper Ranch Group (Massey et al.,



Fig. 1. Bonaparte gold property (red), straddles the boundary between 92I and 92P map sheets (black), near the eastern edge of Quesnel terrane (transparent green overlay). Selected locations of Early Jurassic magmatism: Mount Milligan, porphyry Cu-Au mine; and Cariboo Gold District, gold placer and vein deposits.

2005) which, at this latitude, is basement to Mesozoic volcanic and sedimentary rocks of Quesnel terrane (Fig. 2). The Harper Ranch Group rocks were hornfelsed during emplacement of a composite quartz diorite to monzodiorite porphyritic intrusion

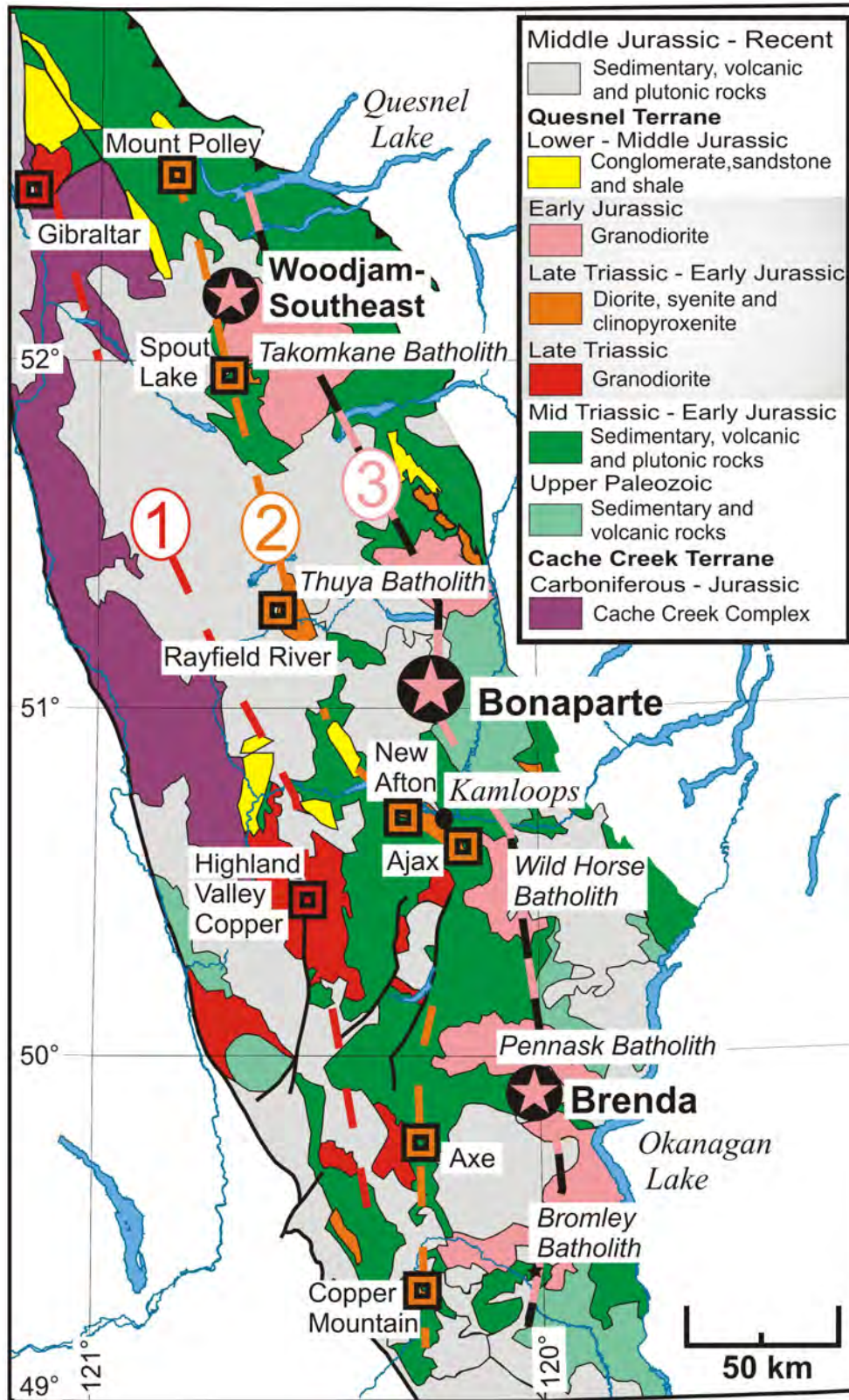


Fig. 2. Generalized geology of southern Quesnellia and Cu-Mo±Au deposits. Mesozoic arc plutons align along the length of southern Quesnellia to define three, north-trending, temporally distinct belts that get younger to the east: 1) Late Triassic; 2) Late Triassic – Early Jurassic; and 3) Early Jurassic. Discrete porphyry copper mineralizing events are directly linked to each of these magmatic episodes. The Bonaparte deposit lies in the tract of Early Jurassic plutons (Wildhorse-Takomkane plutonic suite) midway between the Brenda and Woodjam-Southeast deposits (modified after Massey et al., 2005).

and dike complex, which is mineralized. These intrusive rocks have been correlated with the Early Jurassic Eakin Creek suite of the Late Triassic to Middle Jurassic Thuya batholith (Schiarizza and Israel, 2001; Anderson et al., 2010), which is part of the regional Early Jurassic Wildhorse-Takomkane plutonic suite. Harper Ranch rocks are exposed as inliers near the southeastern margin of an extensive sheet of Chilcotin Group flood basalts (Miocene) that form much of the Bonaparte Plateau.

3. Property geology

The country rock consists of dark, rusty-weathering, polydeformed argillaceous sedimentary rocks of the Harper Ranch Group. At least three discrete intrusive phases are exposed at the “Discovery Zone”: brown quartz diorite, monzodiorite and aplite. All are overprinted by late hydrothermal quartz and quartz-carbonate veins (Fig. 3 in Logan and Mihalynuk, 2013). The quartz diorite is the most intensely foliated, lineated, and altered whereas the monzodiorite is moderately foliated to unfoliated and typically moderately to weakly altered. Aplitic dykes cut both earlier phases and are unfoliated. Based on field relationships Logan and Mihalynuk (2013) interpreted that the quartz diorite is older than the monzodiorite. However, the ages reported herein indicate the reverse.

4. Sample descriptions

To better constrain the timing of the main intrusive phases, we analyzed zircons derived from weakly altered monzodiorite and pervasively biotite-altered quartz diorite porphyry. To estimate the time of mineralization, we analyzed muscovite from alteration zones enveloping mineralized quartz stockworks that cut leucocratic quartz monzonite.

4.1. Monzodiorite, sample 12JLO50-31

A 20 kg sample (12JLO50-31) was collected from a surface trench (Zone 10, UTM 679385E, 5653616N, NAD 83) on the Flicker vein (Fig. 3, Logan and Mihalynuk, 2013). The rock is a weakly propylitically altered, holocrystalline biotite-hornblende monzodiorite (Fig. 3) and is typically medium grained. Quartz comprises ~ 20% of the rock, locally as rounded quartz eyes and matrix. Hornblende and K-feldspar occur as sparse, outsized crystals up to 1 cm long. Up to 10% of the rock is biotite, both as euhedral books and replacements of hornblende. Zircon separated from the monzodiorite yielded clear, colourless, euhedral stubby zircon prisms approximately 200 μ M long.

4.2. Quartz diorite, sample 12JLO50-38

A 20 kg sample of quartz diorite (12JLO50-38) was collected from the Bonaparte trench (Zone 10, UTM 679121E, 5653664N, NAD 83) at the south end of the Crow central vein (Fig. 4, Logan and Mihalynuk, 2013). At this locale, the quartz diorite porphyry (“dark matrix porphyry” of Peatfield, 1986) is pervasively biotite-altered, well foliated and lineated, and hosts disseminated chalcopyrite (Fig. 4). Typically, the diorite is coarse grained and contains white plagioclase (35%),



Fig. 3. Sample 12JLO50-31. Medium-grained equigranular hornblende monzodiorite. Quartz veined and weakly altered to propylitic mineral assemblages of albite, chlorite, epidote \pm pyrite.

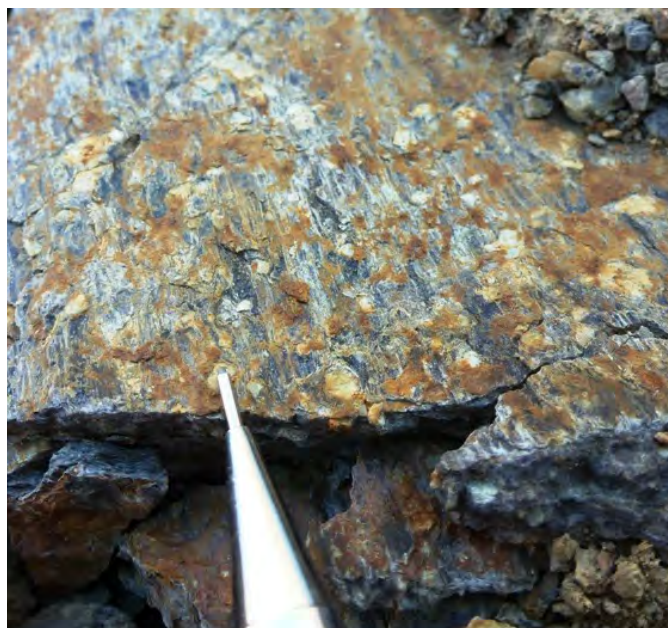


Fig. 4. Sample 12JLO50-38. Strongly foliated and lineated biotite-altered quartz diorite porphyry. Mylonitic fabric is defined by laminae of biotite-quartz-sericite-carbonate and opaque minerals. Equant white grains are plagioclase porphyroclasts. View is down plunge to the east, perpendicular to the northerly trend of the quartz vein.

altered hornblende (5%), distinctive, sparse blue quartz eyes in a fine-grained matrix of prismatic hornblende (20%), and intra-crystalline plagioclase-feldspar \pm quartz containing biotite, apatite, titanite, magnetite and pyrite. The quartz diorite yielded a population of euhedral stubby zircons similar in size and appearance to those from 12JLO50-31.

4.3. Muscovite-quartz-carbonate veins, sample 12JLO50-30x

A muscovite sample (12JLO50-30x) for Ar-Ar step-heating comes from the ore stockpile (Zone 10, 679197E, 5653695N, NAD 83), west of the decline portal (Fig. 3 in Logan and Mihalynuk, 2013). The muscovite forms sub-mm disseminated crystals in bleached, carbonate-sericite alteration envelopes to mineralized quartz stockworks cutting leucocratic quartz monzonite (Fig. 5). Carbonate \pm pyrite introduced along fractures and quartz vein margins has altered and bleached the rock. Sparry calcite fills open spaces between euhedral quartz crystals and is locally accompanied by disseminated arsenopyrite \pm gold, and perhaps, bismuth tellurides (Fig. 5 in Logan and Mihalynuk, 2013).

5. U-Pb and $^{40}\text{Ar}/^{39}\text{Ar}$ geochronology methods

Sample preparation and analytical work was done at the Pacific Centre for Isotopic and Geochemical Research of the Department of Earth, Ocean and Atmospheric Sciences, The University of British Columbia. Details of the mineral separation and analytical techniques are presented in Logan et al. (2007) and Scoates and Friedman (2008).

Zircon was separated from the quartz diorite and quartz monzodiorite samples using standard mineral separation techniques (crushing, grinding, wet shaker Wilfley table, heavy

liquids, and magnetic separation), followed by hand picking. Chemically abraded single zircon grains were analyzed by U-Pb isotope dilution thermal ionization mass spectroscopy (U-Pb ID-TIMS, or simply CA-TIMS). Muscovite and sericite were separated from a leucocratic quartz monzonite phase of the Bonaparte stock and $^{40}\text{Ar}/^{39}\text{Ar}$ isotopic age determinations were obtained from muscovite by laser-induced step-heating.

6. U-Pb geochronology results

U-Pb analyses of chemically abraded single zircon grains separated from the Bonaparte monzodiorite ($n = 4$) and from the quartz diorite porphyry ($n = 4$) are presented in Table 1 and illustrated in Figures 6 and 7.

6.1. Monzodiorite, sample 12JLO50-31

Of the four grains analyzed, two overlap concordia at the 2σ confidence level between 189 and 188 Ma, one lies between 190 and 189 Ma, and one is discordant, lying slightly off concordia at about 191 Ma (Fig. 6, Table 1). The best age estimate for the monzodiorite is from the 2 youngest grains; these give a mean $^{206}\text{Pb}/^{238}\text{U}$ age of 188.8 ± 0.02 Ma, which we take as the age of crystallization.

6.2. Quartz diorite, sample 12JLO50-38

All grains overlap concordia at the 2σ confidence level (Fig. 7, Table 1). Three grains lie between 166 and 165 Ma, and one is centered on 164 Ma. The best age estimate for the quartz diorite is from the three older grains; these give a mean weighted $^{206}\text{Pb}/^{238}\text{U}$ date of 165.9 ± 0.02 Ma, which is taken to be the age of crystallization.

7. $^{40}\text{Ar}/^{39}\text{Ar}$ cooling age, muscovite, sample 12JLO50-30x

Details of the analyses, including gas measurements

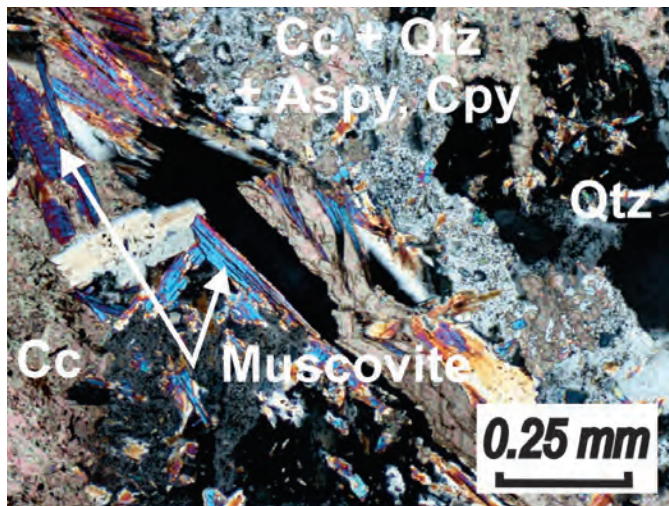


Fig. 5. Photomicrograph of mineralized quartz-carbonate-muscovite vein collected from stockpiled ore. Late-stage calcite and muscovite vein (~ 0.5 mm wide) cuts diagonally across silica- and carbonate-altered quartz diorite (cross polarized light). Disseminated fine needles of arsenopyrite and chalcopyrite are intergrown with calcite. Abbreviations: Qtz, quartz; Cc, calcite; Aspy, arsenopyrite; Cpy, chalcopyrite.

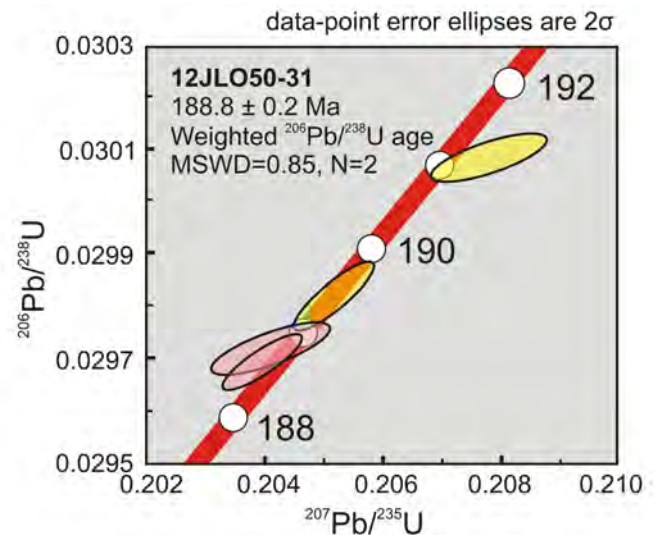


Fig. 6. Concordia plot for U-Pb TIMS data from single zircons, sample 12JLO50-31. Weighted age 188.8 ± 0.2 Ma based on $^{206}\text{Pb}/^{238}\text{U}$ ages of two youngest grains (pink ellipses). Concordia bands include 2σ errors of U decay constants.

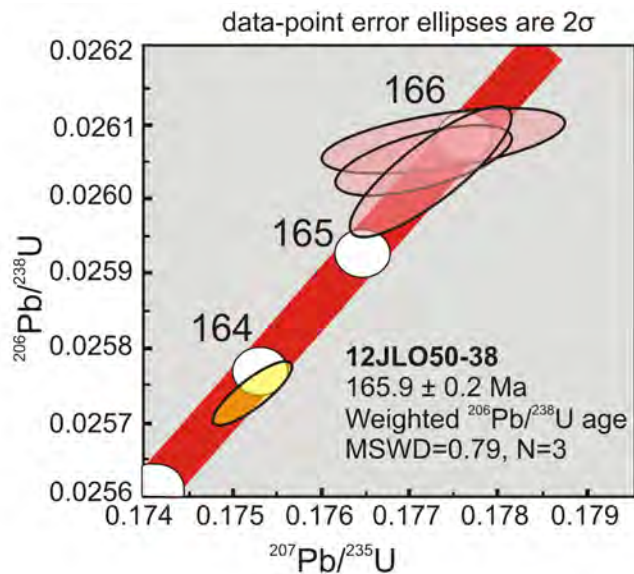


Fig. 7. Concordia plot for U-Pb TIMS data from single zircons, sample 12JLO50-38. Weighted age 165.9 ± 0.2 Ma based on $^{206}\text{Pb}/^{238}\text{U}$ ages of three grains (pink ellipses). Concordia bands include 2σ errors of U decay constants.

obtained during each of the heating steps are presented in Table 2. Initial data entry and calculations were carried out using the software ArArCalc (Koppers, 2002). The plateau and correlation ages were calculated using Isoplot 3.09 (Ludwig, 2003). Errors are quoted at the 2-sigma (95% confidence) level and are propagated from all sources except mass spectrometer sensitivity and age of the flux monitor. Muscovite separated from altered and mineralized leucocratic quartz monzonite yielded a complicated argon release spectra that fails to provide a good plateau cooling age. An inverse isochron plot using seven points yields a correlation age of 160.4 ± 2.4 Ma, an initial $^{40}\text{Ar}/^{39}\text{Ar}$ ratio of 275 ± 42 Ma and a MSWD of 1.18 (Fig. 8, Table 2).

8. Discussion

U-Pb zircon crystallization ages of the Bonaparte intrusions indicate at least two intrusive events, Early Jurassic (~ 189 Ma) and Middle Jurassic (~ 166 Ma). Both are too young to permit correlation with the ~ 195 Ma Wildhorse-Takomkane intrusive suites of Breitsprecher et al. (2010). The biotite-hornblende quartz monzodiorite (sample 12JLO50-31) is ~ 30 m.y. older than the Middle Jurassic porphyritic hornblende quartz diorite (sample 12JLO50-38), which was initially considered the oldest phase in the surface working (Logan and Mihalynuk, 2013).

Early Jurassic intrusive ages similar to the quartz monzonite are known from northern Quesnel terrane at the Mount Milligan porphyry Cu-Au deposit (Jago et al., in press). At Mount Milligan, mineralization is associated with feldspar-pyroxene porphyritic monzonite stocks such as Southern Star ($182.6 + 4.3/- 0.6$ Ma), Heidi Lake (183.0 ± 3 Ma) and North Slope ($189.0 + 3.3/- 1.0$ Ma) and late syn-mineral plagioclase + hornblende porphyritic monzonite dikes (Ghosh, 1992;

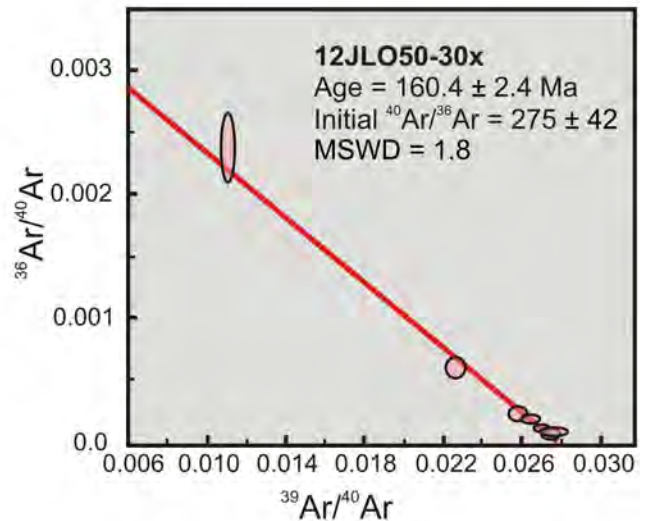


Fig. 8. Inverse isochron plot of step-heating $^{40}\text{Ar}/^{39}\text{Ar}$ analyses for muscovite sample 12JLO50-30x. 2σ error ellipses for individual analytical fractions are pink. Age is 160.4 ± 2.4 Ma with an initial $^{40}\text{Ar}/^{36}\text{Ar}$ of 275 ± 42 Ma.

Mortensen et al., 2005). At Bonaparte however, the biotite-hornblende monzodiorite (~ 189 Ma) is unlikely the cause of mineralization, but rather a host to the younger Middle Jurassic magmatism and associated hydrothermal gold-copper mineralization (~ 160 Ma).

Approximately 200 km north of Bonaparte, Rhys et al. (2009) and Mortensen et al. (2011) reported Jurassic ages for magmatism and mineralization in the Cariboo gold district (Fig. 1), an area that produced 80-97 tonnes of placer gold (Levson and Giles, 1993), roughly half of the total historical gold production in British Columbia. In the Cariboo gold district, at least two stages of quartz veins are known; an early, poorly mineralized and deformed set are cut by later Au-bearing quartz-carbonate-pyritic veins. Laser ablation ICP-MS, zircon crystallization ages from plagioclase \pm quartz \pm hornblende porphyritic sills and dikes at the Spanish Mountain gold deposit yielded ages of 185.6 ± 1.5 to 187 ± 0.8 Ma. The intrusions are deformed and overprinted by late carbonate-fuchsite alteration that is associated with the main mineralization (Rhys et al., 2009). $^{40}\text{Ar}/^{39}\text{Ar}$ geochronology from the Spanish Mountain veins (161-150 Ma) indicates that the mineralization is at least 25 m.y. younger than the intrusions, precluding a direct genetic relationship between the intrusions and mineralization (Mortensen et al., 2011). Similarly, the $^{40}\text{Ar}/^{39}\text{Ar}$ cooling age (~ 160 Ma) of hydrothermal muscovite in the alteration assemblage to vein mineralization at Bonaparte is too young to relate mineralization to intrusion of the ~ 189 Ma quartz monzonite. However ages from the quartz diorite porphyry (~ 166 Ma) imply a link between Au-Cu mineralization and Middle Jurassic intrusion at Bonaparte.

Post-accretion Middle Jurassic plutons in central Quesnellia include the Quesnel River leucogranite (165-158 Ma), Gavin

Table 2. $^{40}\text{Ar}/^{39}\text{Ar}$ step heating gas release data from sample 12JLO50-30x, a muscovite separate from sericite alteration selvage.

| 12JLO50-30x | | Muscovite | | | | | | | | | | |
|---------------|---------------------------------|------------|---------------------------------|------------|---------------------------------|------------|--------|------------------------|--------------------|------------------------------------|--------|------------|
| Laser | Isotope Ratios | | | | | | | | | | | |
| Power (%) | $^{40}\text{Ar}/^{39}\text{Ar}$ | 1 σ | $^{37}\text{Ar}/^{39}\text{Ar}$ | 1 σ | $^{36}\text{Ar}/^{39}\text{Ar}$ | 1 σ | R.I. | % ^{40}Ar atm | f ^{39}Ar | $^{40}\text{Ar}^*/^{39}\text{ArK}$ | Age | 2 σ |
| 2.30 | 90.19 | ± 1.18 | 0.031 | ± 0.45 | 0.214 | ± 0.010 | 0.0332 | 70.04 | 0.58 | 27.023 | 122.10 | ± 26.58 |
| 2.60 | 38.71 | ± 0.27 | 0.004 | ± 0.06 | 0.008 | ± 0.001 | 0.0041 | 6.54 | 8.96 | 36.178 | 161.67 | ± 3.16 |
| 2.90 | 32.74 | ± 0.21 | 0.002 | ± 0.03 | 0.002 | ± 0.000 | 0.0109 | 1.80 | 39.71 | 32.153 | 144.38 | ± 1.87 |
| 3.10 | 36.35 | ± 0.24 | 0.004 | ± 0.05 | 0.002 | ± 0.001 | 0.0014 | 1.60 | 13.56 | 35.772 | 159.93 | ± 2.58 |
| 3.40 | 36.16 | ± 0.37 | 0.007 | ± 0.09 | 0.003 | ± 0.001 | 0.0026 | 2.17 | 13.51 | 35.373 | 158.22 | ± 3.39 |
| 3.80 | 36.98 | ± 0.21 | 0.012 | ± 0.17 | 0.004 | ± 0.000 | 0.0042 | 3.06 | 8.24 | 35.854 | 160.28 | ± 2.07 |
| 4.80 | 37.74 | ± 0.25 | 0.001 | ± 0.01 | 0.007 | ± 0.001 | 0.0103 | 5.19 | 9.90 | 35.783 | 159.98 | ± 2.50 |
| 5.80 | 44.10 | ± 0.40 | 0.003 | ± 0.04 | 0.026 | ± 0.002 | 0.0051 | 17.53 | 5.52 | 36.371 | 162.49 | ± 4.72 |
| Total/Average | 36.99 | ±0.098 | 0.002 | ±0.011 | 0.003 | ± 0.002 | | | 100.00 | 34.826 | | |

J = 0.0025850 ± 0.0000129

Volume ^{39}ArK = 0.083

Integrated Date = 155.92 ± 0.97 Ma

Plateau age = no plateau

Inverse isochron (correlation age) results, plateau steps: Model 1 Solution (±95%-conf.) on 7 points

Age = 160.4 ± 2.4 Ma, Initial $^{40}\text{Ar}/^{36}\text{Ar}$ = 275 ± 42

MSWD = 1.8, Probability = 0.11

Lake porphyritic quartz monzonite (162-160 Ma), Bonaparte Lake granite (164-161 Ma) and in the south, the Osprey Lake batholith (~ 166 Ma). These plutons are locally associated with minor Cu-Au-Mo mineralization (Logan et al., 2007; Logan and Moynihan, 2009) but are generally assumed to be poorly mineralized relative to the Late Triassic and Early Jurassic plutons of Quesnel terrane (Anderson et al., 2010). Geochronologic data presented herein indicate that intrusion-related Au-Cu vein mineralization did form at ~ 160 Ma in this part of Quesnel terrane.

9. Summary and conclusions

Shear-hosted gold-chalcopyrite quartz veins at Bonaparte have produced ~ 103 kg of gold or 25.58 g/t Au from the total 4,064 tonnes shipped (Beaton, 2011). The hypothesis that Bonaparte mineralization is Early Jurassic and analogous to the Brenda Cu-Mo and/or Woodjam Au, Cu-Mo porphyry deposits has been falsified by our geochronologic data. U-Pb zircon crystallization ages for the Bonaparte intrusions indicate at least two separate ages of intrusive activity; Early Jurassic (~ 189 Ma) and Middle Jurassic (~ 166 Ma), and that monzodiorite is the oldest plutonic phase, not quartz diorite as previously suggested (Logan and Mihalynuk, 2013). Muscovite from quartz-carbonate-sericite alteration associated with late-stage copper-arsenopyrite-gold mineralization yielded a cooling age of 160.4 ± 2.42 Ma, linking the bulk of mineralization to the younger, Middle Jurassic episode of magmatism. Both intrusions are younger than the ~ 195 Ma Wildhorse-Takomkane intrusive suite, ruling out correlation.

References cited

Anderson, R.G., Schiarizza, P., Andrews, G., Breitsprecher, K., Davis, W., Dunne, C.E., Plouffe, A., and Thomas, M.D., 2010.

Bedrock, surficial, geophysical and geochemical mapping reveals exploration targets in the Thuya batholith, southern Nicola arc. In: Geological Association of Canada, Targeted Geoscience Initiative 3 Workshop, March 2010, Vancouver, 52-57. URL accessed November, 2012, http://www.gac-cs.ca/workshops/TGI3/abstracts/GAC_TGI3_workshop_abstracts.pdf.

Beaton, A.J., 2011. Bonaparte gold underground decline and surface trench bulk-sample project. British Columbia Ministry of Energy, Mines and Petroleum Resources, Assessment report #32,930, 382 p.

Breitsprecher, K., Weis, D., Scoates, J.S., and Anderson, R.G., 2010. Targeting mineralized Late Triassic to Early Jurassic plutons in the Nicola arc, southern Quesnel terrane, Canadian Cordillera. In: Geological Association of Canada, Targeted Geoscience Initiative 3 Workshop, Vancouver, 49-51. URL accessed November, 2012, http://www.gac-cs.ca/workshops/TGI3/abstracts/GAC_TGI3_workshop_abstracts.pdf.

Crowley, J.L., Schoene, B., and Bowring, S.A., 2007. U-Pb dating of zircon in the Bishop Tuff at the millennial scale. *Geology*, 35, 1123-1126.

Durfeld, R., 1980. Geology report on the JS mineral claim. British Columbia Ministry of Energy, Mines and Petroleum Resources, Assessment report #8,500, 11 p.

Gerstenberger, H., and Haase, G., 1997. A highly effective emitter substance for mass spectrometric Pb isotopic ratio determinations. *Chemical Geology*, 136, 309-312.

Ghosh, D., 1992. Uranium-lead zircon geochronometry and isotope geochemistry. In: Copper-Gold porphyry systems of British Columbia: University of British Columbia, Mineral Deposits Research Unit, Annual Technical Report, Year One, July 1991-June 1992, 12.1-12.11.

Jaffey, A.H., Flynn, K.F., Glendenin, L.E., Bentley, W.C., and Essling, A.M., 1971. Precision measurement of half-lives and specific activities of ^{235}U and ^{238}U . *Physical Review*, C4, 1889-1906.

Jago, C.P., Tosdal, R.M., Cooke, D.R., and Harris, A.C., in press.

- Vertical and lateral variation of mineralogy and chemistry in the Early Jurassic Mt. Milligan alkalic porphyry Au-Cu deposit, British Columbia, Canada. *Economic Geology*, 108.
- Koppers, Anthony A.P., 2002. ArArCALC – software for $^{40}\text{Ar}/^{39}\text{Ar}$ age calculations. *Computers and Geosciences* 28 (2002), 605-619.
- Kuiper, K.F., Deino, A., Hilgen, F.J., Krijgsman, W., Renne, P.R., and Wijbrans, J.R., 2008. Synchronizing rock clocks of earth history. *Science*, 320, 500-504.
- Leitch, C.H.B., 1988. A polished section and SEM study of Bi- and precious metal tellurides from the Discovery Zone, Bonaparte property. British Columbia Ministry of Energy, Mines and Petroleum Resources, Assessment report #17,206, 380 p.
- Levson, V.M., and Giles, T.R., 1993. Geology of Tertiary and Quaternary gold-bearing placers in the Cariboo region, British Columbia (93A, B, G, H). British Columbia Ministry of Energy, Mines and Petroleum Resources, Bulletin 89, 202 p.
- Logan, J.M., and Mihalynuk, M.G., 2013. Bonaparte gold: another 195 Ma Au-Cu porphyry deposit in southern British Columbia? In: *Geological Fieldwork 2012*, British Columbia Ministry of Energy, Mines and Natural Gas, British Columbia Geological Survey Paper 2013-1, 71-80.
- Logan, J.M., and Moynihan, D.P., 2009. Geology and mineral occurrences of the Quesnel River map area, central British Columbia (NTS 093B/16). In: *Geological Fieldwork 2008*, British Columbia Ministry of Energy and Mines, British Columbia Geological Survey Paper 2009-1, 127-152.
- Logan, J.M., Mihalynuk, M.G., Ullrich, T., and Friedman, R.M., 2007. U-Pb ages of intrusive rocks and $^{40}\text{Ar}/^{39}\text{Ar}$ plateau ages of copper-gold-silver mineralization associated with alkaline intrusive centres at Mount Polley and the Iron Mask Batholith, southern and central British Columbia. In: *Geological Fieldwork 2006*, British Columbia Ministry of Energy, Mines and Petroleum Resources, British Columbia Geological Survey Paper 2007-1, 93-116.
- Logan, J.M., Mihalynuk, M.G., Friedman, R.M., and Creaser, R.A., 2011. Age constraints of mineralization at the Brenda and Woodjam Cu-Mo±Au porphyry deposits – an Early Jurassic calc-alkaline event, south-central British Columbia. In: *Geological Fieldwork 2010*, British Columbia Ministry of Forests, Mines and Lands, British Columbia Geological Survey Paper 2011-1, 129-144.
- Ludwig, K.R., 2003. *Isoplot 3.09: a geochronological toolkit for Microsoft Excel*. Berkeley Geochronology Center Special Publication, 4, 70 p.
- Massey, N.W.D., MacIntyre, D.G., Desjardins, P.J., and Cooney, R.T., 2005. Digital geology map of British Columbia: whole province. British Columbia Ministry of Energy, Mines and Petroleum Resources, GeoFile 2005-1.
- Mattinson, J.M., 2005. Zircon U-Pb chemical abrasion (“CA-TIMS”) method: combined annealing and multi-step partial dissolution analysis for improved precision and accuracy of zircon ages. *Chemical Geology*, 220, 47–66.
- Mortensen, J.K., Ghosh, D.K., and Ferri, F., 1995. U-Pb geochronology of intrusive rocks associated with copper-gold porphyry deposits in the Canadian Cordillera. In: *Porphyry Deposits of the northwestern Cordillera of North America*, Schroeter, T.G., ed., Canadian Institute of Mining, Metallurgy and Petroleum Special Volume 46, 142–158.
- Mortensen, J.K., Rhys, D.A., and Ross, K., 2011. Investigations of orogenic gold deposits in the Cariboo gold district, east-central British Columbia (parts of NTS 093A, H): final report. In: *Geoscience BC Summary of Activities 2010*, Geoscience BC, Report 2011-1, 97–108.
- Mundil, R., Ludwig, K.R., Metcalfe, I., and Renne, P.R., 2004. Age and timing of the Permian mass extinctions: U/Pb dating of closed-system zircons. *Science*, 305, 1760-1763.
- Peatfield, G.R., 1986. Geology, rock and soil geochemistry, geophysics and diamond drilling on the Bob 1986 group (Bonaparte property). British Columbia Ministry of Energy, Mines and Petroleum Resources, Assessment report #15,166, 308 p.
- Rhys, D.A., Mortensen, J.K., and Ross, K., 2009. Investigations of orogenic gold deposits in the Cariboo gold district, east-central British Columbia (parts of NTS 093A, H): progress report. In: *Geoscience BC Summary of Activities 2008*, Geoscience BC, Report 2009-1, 49–74.
- Schiarizza, P., and Israel, S., 2001. Geology and mineral occurrences of the Nehalliston Plateau, south-central British Columbia (92P/7, 8, 9, 10). In: *Geological Fieldwork 2000*, British Columbia Ministry of Energy, Mines and Petroleum Resources, British Columbia Geological Survey Paper 2001-1, 1-30.
- Scoates, J.S., and Friedman, R.M., 2008. Precise age of the platinumiferous Merensky Reef, Bushveld Complex, South Africa, by the U-Pb ID-TIMS chemical abrasion ID-TIMS technique. *Economic Geology*, 103, 465-471.
- Schmitz, M.D., and Schoene, B., 2007. Derivation of isotope ratios, errors, and error correlations for U-Pb geochronology using ^{205}Pb - ^{235}U -(^{233}U)-spiked isotope dilution thermal ionization mass spectrometric data. *Geochemistry, Geophysics, Geosystems*, 8, Q08006, doi:10.1029/2006GC001492.
- Stacey, J.S., and Kramers, J.D., 1975. Approximation of terrestrial lead isotopic evolution by a two-stage model. *Earth and Planetary Science Letters*, 26, 207–221.
- Thirlwall, M.F., 2000. Inter-laboratory and other errors in Pb isotope analyses investigated using a ^{207}Pb - ^{204}Pb double spike. *Chemical Geology*, 163, 299-322.